The accuracy of modal parameters estimation for highway bridges influenced by various ambient vibrations

Md. Rajab Ali, Takatoshi Okabayashi and Toshihiro Okumatsu
Department of Civil Engineering, Nagasaki University, Nagasaki, Japan

ABSTRACT: This paper explains about the influence of ambient vibration characteristics in estimating the modal parameters (frequency, damping constant, and vibration mode) of highway bridges using balanced stochastic realization (BSR-I and BSR-II) theories. Ambient vibration experiments were conducted on the Kabashima Bridge (an arch bridge of length 136m, and situated in Nagasaki city) to obtain the ambient vibration data induced by wind, and running vehicle. The measurement data are then analyzed by using balanced stochastic realization theories and the modal parameters are estimated as well. The obtained results reveal that wind excited vibration data gives better estimation accuracy. In contrast, vibration data obtained under traffic excitation offers some lacks in estimation accuracy for lower mode frequencies. In this case, the higher mode frequencies are easily inducing due to the influence of moving automobile but estimation accuracy declines as well. Furthermore, the identified results, demonstrated that the BSR-II method realizes better results than the BSR-I method. Based on the findings, it can be recommended that while executing the vibration experiment, the automobiles interaction should be avoided or modeling of the moving vehicle could be considered in the analysis process in order to estimate the modal parameters of highway bridges accurately.

1 INTRODUCTION

The recent advances in communications technology and in personal computers in conjunction with improved measurement technology have made it more realistic to contemplate monitoring the dynamic behavior of highway bridges in remote areas. Highly accurate estimates of highway bridge modal parameters (natural frequencies, damping constants, and vibration modes) are now possible through the application of realization theories to highway bridge excitation under wind and moving vehicle loadings (Gever 2006). There is now an urgent need to bring these together in a technology for investigating bridge deterioration and damage based on monitored vibration information.

A useful method of identifying damage and deterioration in highway bridges, which gives highly accurate results, is to automatically estimate the structural modal parameters under ambient vibration. In addition to the modal analysis and ARMA model (Carden 2008, Garibaldi 1998 et al, and Papakos et al. 2003), realization theories have been proposed as part of the control theory (Juang 1994), giving rise to major advances in research on estimating the bridge dynamic characteristics. In this approach, the dynamic properties are estimated from the transfer function or the impulse response function obtained using input-output data for the structure.

For large-scale civil structures, such as, long-span highway bridges, it is difficult to implement the vibration tests using artificial forces. In contrast, the large surface area of a bridge makes it susceptible to wind interactions leading to long-time vibrations. These vibrations are assumed to be similar to the stationary response of a structure under white noise excitation, and, are modeled as stochastic processes. When this approach of characterization is adopted, only the output data is required to estimate the structural modal parameters.

Akaike proposed a method for estimating the state space model from the canonical correlation of a stochastic process (Akaike 1976). Successive extension of this theory has been introduced based on the techniques of estimating the system matrices. Aoki (Aoki 1987) estimated the system matrices using canonical correlations between the future and past

observations whereas; the system matrices (A and C) are also possible to be estimated from the identified state vector (Overschee 1996). The approaches correspond to BSR-I, and BSR-II method respectively. These methods provide protection against noisy data since they adopt several robust numerical techniques, such as, the LQ decomposition, the SVD, and the least-squares method. Due to their remarkable advantages, these theories have been effectively applied to simulated and real structural data (Abdelghani et al. 1998, Baseville et al. 2001, Lardies 1998, Magalhães et al. 2009, and Peeters et al. 2001). However, a few studies have considered the influence of the ambient vibration behavior, particularly, for the wind velocity and moving vehicle on the estimation accuracy. This aspect still remains as a significant challenge to researchers.

This paper explains about the influence of ambient vibration characteristics in estimating the modal parameters (frequency, damping constant, and vibration mode) of highway bridges using balanced stochastic realization (BSR-I and BSR-II) theories. Ambient vibration experiment was conducted on the Kabashima Bridge (an arch bridge of length 136m, and situated in Nagasaki city) to obtain the ambient vibration data induced by wind, and running vehicle. The measurement data are then analyzed by using balanced stochastic realization theories and the influence of ambient vibration on the modal parameters estimation accuracy were investigated.

2 STRUCTURE MODELING

The dynamic behavior of a highway bridge is modeled using a finite element method. It is expressed by an *n*-dof system equation of motion

$$m\ddot{z}(t) + c\dot{z}(t) + kz(t) = dw(t) \tag{1}$$

where $\mathbf{z}(t) \in \mathbf{R}^{2n}$ is the displacement and $\mathbf{w}(t) \in \mathbf{R}^{r}$ is the external force. Terms $\mathbf{m} \in \mathbf{R}^{n\times n}$, $\mathbf{c} \in \mathbf{R}^{n\times n}$, $\mathbf{k} \in \mathbf{R}^{n\times n}$, and $\mathbf{d} \in \mathbf{R}^{n\times r}$ are the mass, general viscous damping, stiffness matrix, and external force acting on the r^{th} node of the bridge.

For sampling time *T* and a zero-order hold assumption, the external force $\mathbf{w}(t)$ and state variable $\mathbf{x}(t)$ are constants over the interval $t_k \le \tau \le t_{k+1} = t_k + T$.

$$\mathbf{w}(t) = \mathbf{w}(k) \ , \ \mathbf{x}(t) = \mathbf{x}(k) \tag{2}$$

Consequently, the state variable of the structure $\mathbf{x}(k) \in \mathbf{R}^{2n}$ for discretre time is defined as

$$\mathbf{x}(t) = \begin{bmatrix} \mathbf{z}(k) \\ \dot{\mathbf{z}}(k) \end{bmatrix} \tag{3}$$

Hence, Eq.(1) can be rearranged into discretized form as

$$\mathbf{x}(k+1) = \mathbf{A}\mathbf{x}(k) + \mathbf{B}\mathbf{w}(k) \tag{4a}$$

$$\mathbf{y}(k) = \mathbf{C}\mathbf{x}(k) \tag{4b}$$

where $\mathbf{y}(k) \in \mathbf{R}^{m}$ is the *m*-point observation data. The coefficient matrices $\mathbf{A} \in \mathbf{R}^{2n\times 2n}$ and $\mathbf{B} \in \mathbf{R}^{2n\times r}$ are as follows

$$\mathbf{A} = e^{\overline{\mathbf{A}}T} \ , \ \mathbf{B} = (e^{\overline{\mathbf{A}}T} - \mathbf{I})\overline{\mathbf{A}}^{-1}\overline{\mathbf{B}} \tag{5}$$

where the system matrix $\overline{\mathbf{A}} \in \mathbf{R}^{2n\times 2n}$ and force matrix $\overline{\mathbf{B}} \in \mathbf{R}^{2n\times r}$ have the definition and $\mathbf{C} \in \mathbf{R}^{m\times 2n}$ is the observation matrix.

$$\overline{\mathbf{A}} = \begin{bmatrix} \mathbf{c} & \mathbf{m} \\ \mathbf{m} & \mathbf{0} \end{bmatrix}^{-1} \begin{bmatrix} -\mathbf{k} & \mathbf{0} \\ \mathbf{0} & \mathbf{m} \end{bmatrix}, \quad \overline{\mathbf{B}} = \begin{bmatrix} \mathbf{c} & \mathbf{m} \\ \mathbf{m} & \mathbf{0} \end{bmatrix}^{-1} \begin{bmatrix} \mathbf{d} \\ \mathbf{0} \end{bmatrix} \tag{6}$$

3 STOCHASTIC REALIZATION THEORY

3.1 Basic formulation

Consider $\{\mathbf{y}(t), t = 1, 2, \ldots N + 2k - 2\}$ as the measured data over finite time for sufficiently large values of N with k>0 and $\mathbf{y}(k)$ as the measurement data for present time t. In this condition, the past and future response data blocks are to be $\mathbf{Y}_p \in \mathbf{R}^{mk \times N}$ and $\mathbf{Y}_f \in \mathbf{R}^{mk \times N}$. Then, the auto covariance and orthogonal covariance of $\mathbf{Y}_p$ and $\mathbf{Y}_f$ are obtained, as follows:

$$\begin{bmatrix} \mathbf{\Sigma}_{pp} & \mathbf{\Sigma}_{pf} \\ \mathbf{\Sigma}_{fp} & \mathbf{\Sigma}_{ff} \end{bmatrix} = \frac{1}{N} \begin{bmatrix} \mathbf{Y}_p \\ \mathbf{Y}_f \end{bmatrix} \begin{bmatrix} \mathbf{Y}_p^T & \mathbf{Y}_f^T \end{bmatrix} \tag{7}$$

where $\mathbf{\Sigma}_{pp}$, $\mathbf{\Sigma}_{fp}$, $\mathbf{\Sigma}_{ff}$ are finite dimensional approximations over the infinite dimensional Hankel matrix $\mathbf{H}$ and Toeplitz matrices $\mathbf{T}_+$, $\mathbf{T}_-$ respectively that are obtained by LQ decomposition of the right side of Eq.(7).

3.2 Balanced Stochastic Realization (BSR-I) method

Using full rank factorization, square root matrices of the covariance matrices $\mathbf{\Sigma}_{ff}$ and $\mathbf{\Sigma}_{pp}$ are estimated that satisfy the following conditions:

$$\mathbf{\Sigma}_{ff} = \mathbf{L}\mathbf{L}^T, \quad \mathbf{\Sigma}_{pp} = \mathbf{M}\mathbf{M}^T \tag{8}$$

The Singular Value Decomposition (SVD) of the normalized covariance matrix $\mathbf{\Sigma}_{fp}$ yields the equation below.

$$\mathbf{L}^{-1}\mathbf{\Sigma}_{fp}\,\mathbf{M}^{-T} = \mathbf{U}\mathbf{\Sigma}V^T = \mathbf{U}_s\mathbf{\Sigma}_s\mathbf{V}_s^T \tag{9}$$

where, $\mathbf{\Sigma}_s$ is obtained by discarding values of $\mathbf{\Sigma}$ that are too small. The dimension of the state vector is $s = \dim \mathbf{\Sigma}_s$. The extended observability and controllability matrices are then be defined by the relations below.

$$\mathbf{P}_k = \mathbf{L}\mathbf{U}_s\mathbf{\Sigma}_s^{\frac{1}{2}}, \quad \mathbf{Q}_k = \mathbf{\Sigma}_s^{\frac{1}{2}}\mathbf{V}_s^T\mathbf{M}^T \tag{10}$$

Using Eq.(10), matrices $\mathbf{A}$, $\mathbf{C}$, and $\mathbf{B}$ are estimated as

$$\mathbf{A} = \underline{\mathbf{P}}_k^+ \overline{\mathbf{P}}_k, \quad \mathbf{C} = \mathbf{P}_k(1:m,:), \quad \mathbf{B}^T = \mathbf{Q}_k(:,1:m) \tag{11}$$

where, $\underline{\mathbf{P}}_k = \mathbf{P}_k(1:m,:)$ and $\overline{\mathbf{P}}_k = \mathbf{P}_k(m+1:km,:)$ are the matrices formed by excluding the lower and upper m rows of $\mathbf{P}_k$.

3.3 Subspace Stochastic Realization (BSR-II) method

Using Eqs.(7), (8), and (10) we can estimate the s-dimensional state vector as

$$\overline{\mathbf{X}}_k = \mathbf{Q}_k\mathbf{\Sigma}_{pp}^{-1}\mathbf{Y}_p = \mathbf{\Sigma}_s^{\frac{1}{2}}\mathbf{V}_s^T\mathbf{M}^{-1}\mathbf{Y}_p \text{ and } \hat{\mathbf{X}}_{k+1} = \overline{\mathbf{X}}_k(:, 2:N) \tag{12}$$

where, $\hat{\mathbf{X}}_{k+1} = \overline{\mathbf{X}}_{k+1} \in \mathbf{R}^{s \times (N-1)}$ is the state vector at time k+1 that is calculated with the N-1 columns of $\overline{\mathbf{X}}_k \in \mathbf{R}^{s \times N}$. Accordingly,

$$\mathbf{Y}_{k/k} = [\mathbf{y}(k) \quad \Lambda \quad \Lambda \quad \mathbf{y}(k+N-1)] \text{ and } \hat{\mathbf{Y}}_{k/k} = \mathbf{Y}_{k/k}[\mathbf{y}(k) \quad \Lambda \quad \Lambda \quad \mathbf{y}(k+N-1)] \tag{13}$$

The following relations are then calculated using the least squares method:

$$\begin{bmatrix} \hat{\mathbf{X}}_{k+1} \\ \hat{\mathbf{Y}}_{k/k} \end{bmatrix} = \begin{bmatrix} \mathbf{A} \\ \mathbf{C} \end{bmatrix} \hat{\mathbf{X}}_k + \begin{bmatrix} \boldsymbol{\rho}_w \\ \boldsymbol{\rho}_v \end{bmatrix} \quad ((s+m)\times(N-1)) \quad \text{or} \quad \begin{bmatrix} \mathbf{A} \\ \mathbf{C} \end{bmatrix} = (\begin{bmatrix} \hat{\mathbf{X}}_{k+1} \\ \hat{\mathbf{Y}}_{k/k} \end{bmatrix} \hat{\mathbf{X}}_k)(\hat{\mathbf{X}}_k \hat{\mathbf{X}}_k{}^T)^{-1} \tag{14}$$

where, $\boldsymbol{\rho}_w \in \mathbf{R}^s$ and $\boldsymbol{\rho}_v \in \mathbf{R}^m$ are the estimation errors to be considered as white noise.

Thus, the coefficient matrices **A** and **C** can be estimated.

3.4 Dynamic characteristics estimation

The eigenvalue analysis of coefficient matrix **A** (which is derived in Eqs. (11), and (14)) generates the dynamic properties of the system. Frequencies and damping constants are obtained from the real and imaginary part of complex eigenvalues as such

$$h_k \omega_k = -1/\Delta \log \sqrt{X_{\mathrm{Re}}^k{}^2 + X_{\mathrm{Im}}^k{}^2}, \quad \omega_k \sqrt{1-h_k^2} = 1/\Delta \tan^{-1}(X_{\mathrm{Im}}^k / X_{\mathrm{Re}}^k) \tag{15}$$

where, Δ is data sampling time. The vibration mode $\hat{\boldsymbol{\Phi}} \in \mathbf{C}^{m\times 2n}$ is found from $\boldsymbol{\Phi} \in \mathbf{C}^{2n\times 2n}$ as

$$\hat{\boldsymbol{\Phi}} = \mathbf{C}\boldsymbol{\Phi} \tag{16}$$

3.5 Parameter estimation

As noted in relation to Eq.(7), the size of *N* and *k* has a significant effect on estimation accuracy. If the values of N and *k* are too small, poor accuracy results, whereas selection of large values increases the size of the Hankel and Toeplitz matrices leading to significantly higher computational load. Consequently, it is crucial that the Hankel and Toeplitz matrices are of the optimum size. Besides, the length of the singular value *s* introduced in Eq.(9) has to be considered carefully. From the physical appearance of singular values, it is clear that zero or near zero singular values should be discarded. We then optimized the size of H and T matrices and the singular value for use in the estimation process by a trial and error method.

4 AMBIENT VIBRATION MEASUREMENTS

4.1 The Kabashima Bridge and experiments

The structure selected for measurement of ambient vibration was the Kabashima Highway Bridge, built in 1986 and located in Nagasaki city. It is a arch bridge with a maximum span of 153m, a total length of 227m, and a width of 7.5m. Fig.1 shows a general view of the bridge and instrumentation during the experiment. Five sensors affixed along the bridge axis at equal intervals, with one sensor at bridge midpoint. The instruments used for the experiments are listed on Table 1. Data were recorded at the rate of 100 samples per second. The measurement was conducted in different time under windy, and moving vehicle conditions. The acceleration signals is converted from analogue to digital data by AD converter card (DAQ Card), and recor-ded by the personal computer. Modal parameters (frequencies, damping constants, and vibration modes) were estimated from the automatically collected ambient vibration data by offline processing.

Figure 1 : Ambient vibration measurement on Kabashima Bridge

Table 1 : Bridge Instrumentation for experiments

Devices	Type (manufactured)	Specification
A/D converter	DAC card-6062E (NI)	Analogue Input: 16ch, 2bit
Accelerometer	710 (TEAC)	Sensitivity: 300(mv/m/s^2), frequency response: 0.02-200Hz
Amplifier	SA-611 (TEAC)	-
Note PC	CF-19 (Panasonic)	OS: Windows XP Pro

(a) (b)

Figure 2 : Vibration data measured under windy conditions and the power spectrum density: (a) Windy data, (b) Power spectrum density

(a) (b)

Figure 3 : Vibration data measured under moving vehicle and the power spectrum density: (a) Moving vehicle data, (b) Power Spectrum Density

4.2 Measured ambient vibration data

As already described, two main options were considered for measurement condition. The first was to choose vibrations induced by winds, whereas the second option was to select data for moving vehicle. In this study, these two samples are referred to as windy and moving vehicle induced ambient vibration data, respectively. Fig.2(a) and 2(b) show the wind response and related power spectrum density, respectively. The data presented in Fig.3(a) is the response measured under moving vehicle excitation, while Fig.3(b) shows the related power spectrum density.

4.3 Overall considerations on calculation process

For the calculation process, we considered the optimum size of N and k to be (5×200) and (5×40) respectively. One thousand two hundred (1200) data points were analyzed to estimate each set of modal parameters and calculations were continued 25 times. The two different

ambient vibration data samples were used to perform the estimation process by the BSR-I, and BSR-II method. The estimated results ate discussed in the section 5 and 6 as well.

5 MODAL PARAMETERS ESTIMATION ACCURACY BY BSR-I METHOD

5.1 Frequencies

Frequencies are estimated by the BSR-I method from the two types of ambient vibration data sample; the results obtained from the windy data are shown in Fig.4(a). This demonstrates that frequencies for the first through seventh modes are estimated regularly. However, estimated frequencies above 4Hz appear to be more scattered and cannot be separated clearly. On the other hand, with the moving vehicle data, the frequencies above 4Hz are estimated more consistently since moving vehicle can induce the higher modes easily. To illustrate this, Table 2 compares estimation accuracy for windy and moving vehicle data. The coefficient of variation (C.V.) is lower up to the fifth mode, whereas it is higher for sixth, and seventh modes in the case of windy data. This signifies that better accuracy can be realized using windy data especially lower mode frequencies. Contrastingly there is some lacks in estimation accuracy for the result obtained from the moving vehicle data.

5.2 Damping constants

Following a similar process, the damping constants estimation accuracy is evaluated. The results obtained using the windy data are presented in Fig.4(b). As above, the accuracy of these estimates is compared in Table 2. The general conclusion to be drawn from this figure and table is that damping constants estimates are of considerably lower accuracy than the frequencies estimates; the C.V. value has a range 98-170%. This conclusion is consistent with the accepted understanding that estimated damping constants are usually not as accurate as frequencies. Comparatively higher values of damping constants for the first mode are estimated from the windy data. The possible causes might be due to the effect of external force (high wind force) on the systems damping properties.

5.3 Vibration modes

Vibration modes are estimated by the BSR-I methods both windy and moving vehicle data samples and has been shown in Fig.4 (c). These vibration modes plots are the averages of 25 estimates. The estimated first, second, third, and fifth mode vibrations are similar in shape to the modes of a typical arch bridge. The fourth mode is identical with the second mode and can be considered as torsion mode. Although the sixth and seventh modes are estimated, they are not symmetrical like a standard vibration modes. This is because the number of measurement points (five) is less than the mode number (seven).

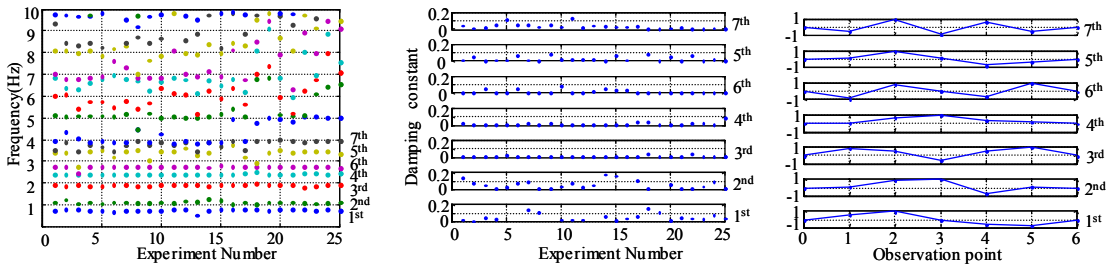

(a) (b) (c)

Figure 4 : Modal parameters estimated from windy data (BSR-I method): (a) Frequencies, (b) Damping constant, (c) Vibration modes

Table 2 : Accuracy evaluation for estimated bridge dynamic characteristics (BSR-I method).

Mode order	Experiment condition	Estimated frequencies (Hz)			Estimated Damping constant		
		Mean	Std.	C.V.	Mean	Std.	C.V.
1st	Windy	0.766	0.562	7.34	0.1166	0.1931	165.64
	Moving vehicle	0.827	0.1005	12.16	0.0371	0.0592	159.66
2nd	Windy	1.129	0.0594	5.26	0.0789	0.0993	125.86
	Moving vehicle	1.241	0.2838	22.87	0.2074	0.2037	98.21
3rd	Windy	1.908	0.0315	1.65	0.0091	0.0113	124.83
	Moving vehicle	1.959	0.1806	9.22	0.0328	0.0847	258.20
4th	Windy	2.426	0.0259	1.07	0.0141	0.0187	132.80
	Moving vehicle	2.562	0.1190	4.65	0.0182	0.0181	99.48
5th	Windy	2.756	0.0607	2.20	0.0185	0.0232	125.14
	Moving vehicle	2.849	0.2112	7.41	0.0377	0.0682	181.05
6th	Windy	3.402	0.2197	6.46	0.0366	0.0515	140.60
	Moving vehicle	3.339	0.1926	5.77	0.0673	0.1140	169.29
7th	Windy	3.800	0.1768	4.65	0.0336	0.0332	98.94
	Moving vehicle	3.659	0.2593	7.09	0.0317	0.0508	160.45

6 MODAL PARAMETERS ESTIMATION ACCURACY BY BSR-II METHOD

6.1 Frequencies

Vibration frequencies are estimated both for windy and moving vehicle data by the BSR-II method. Results from the windy data are given in Fig.5(a). This shows that frequencies from the first through seventh modes are estimated with a good level of consistency, whereas frequencies above 4Hz cannot be clearly separated since the results deviate too much among estimates. A comparison of the results from windy and moving vehicle data samples is presented in Table 3. This reveals that the coefficient of variation for the windy sample is within 4.15% up to fourth mode. The C.V. for the result from moving vehicle data is significantly higher for first and second mode and this value is decreasing as the number of mode increases. Based on the results in Table 2 and 3, it is clear that the BSR-II method offers better estimation accuracy as compared with the BSR-I method.

6.2 Damping constants

Damping constants estimated from the windy data sample are presented in Fig.5(b). There is some scatter in estimated damping constants for first and second modes, but there is more consistent than in the results obtained with the BSR-I method. For comparison, estimated values are given in Table 3, which reveals that there is no big difference in realized C.V. for windy and moving vehicle data.

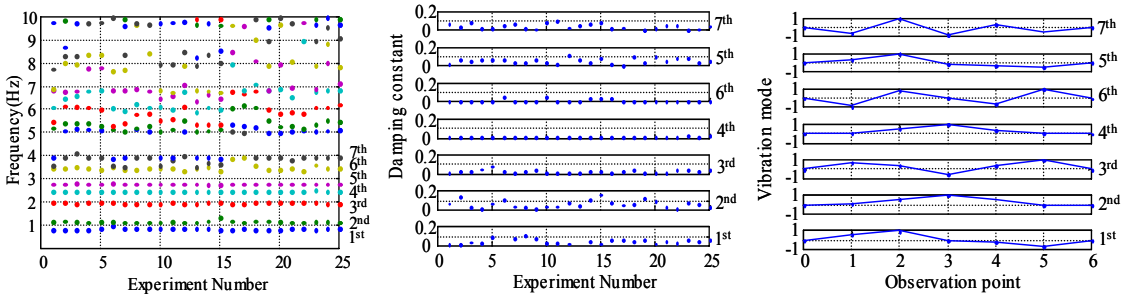

(a) (b) (c)

Figure 5 : Modal parameters estimated from windy vibration data (BSR-II method): (a) Frequencies, (b) Damping constant, (c) Vibration modes

Table 3 : Accuracy evaluation for estimated bridge dynamic characteristics (BSR-II method).

Mode order	Experiment condition	Estimated frequencies (Hz)			Estimated Damping constant		
		Mean	Std.	C.V. (%)	Mean	Std.	C.V. (%)
1st	Windy	0.821	0.0269	3.28	0.0605	0.0546	90.21
	Moving vehicle	0.843	0.0764	9.07	0.0763	0.0768	100.59
2nd	Windy	1.138	0.0405	3.56	0.0612	0.0427	69.71
	Moving vehicle	1.200	0.0720	6.00	0.0549	0.0492	89.70
3rd	Windy	1.937	0.0141	0.73	0.0242	0.0167	68.79
	Moving vehicle	1.873	0.0148	0.79	0.0205	0.0156	76.46
4th	Windy	2.427	0.0114	0.47	0.0065	0.0058	89.09
	Moving vehicle	2.423	0.0280	1.15	0.0322	0.0191	59.31
5th	Windy	2.761	0.0092	0.33	0.0140	0.0161	115.12
	Moving vehicle	2.767	0.0192	0.69	0.0117	0.0095	81.21
6th	Windy	3.481	0.1443	4.15	0.0576	0.0272	47.10
	Moving vehicle	3.403	0.0670	1.97	0.0398	0.0226	56.67
7th	Windy	3.915	0.3777	9.65	0.0414	0.0338	81.75
	Moving vehicle	3.546	0.1748	4.93	0.0294	0.0178	60.63

6.3 Vibration modes

Vibration modes are estimated by the BSR-II methods both windy and moving vehicle data samples. The estimated vibration modes obtained by the BSR-II method from the windy data sample are presented in Fig.5(c). This figure reveals that the estimated vibration modes similar in shape with those estimated from BSR-I method.

7 CONCLUSIONS

In this study, two different types data measured under windy and moving vehicle condition were analyzed to investigate the influence of ambient vibration characteristics on modal parameters estimation accuracy. The investigation results lead to the following conclusions.

(1) The results obtained with ambient vibration data under windy and moving vehicle condition show distinct variations that prove the influence of data characteristics on estimation accuracy. In particular, better estimation accuracy is realized from windy ambient vibration data;

(2) There is some lacks or deficiency in estimation accuracy for the data measured under moving vehicle condition. Contrary, the estimation accuracy improves for higher mode frequency as compared to windy data signifies the moving vehicle's influence on estimation accuracy;

(3) The BSR-II method gave better estimation accuracy than the BSR-I method. Based on the findings, it can be recommended that while executing the vibration experiment, the automobiles interaction should be avoided or modeling of the moving vehicle could be considered in order to estimate the modal parameters of highway bridges accurately.

REFERENCES

Abdelghani, M. et al. 1998. Comparison study of subspace identification methods applied to flexible structures, Mechanical Systems and Signal Processing 12(5):p.679-692.

Akaike, H. 1976. Canonical correlation analysis of time series and the use of an information criterion, in system identification: Advances and Case Studies, Academic, p.27-96.

Aoki, M. 1987. State space modeling of time series, Springer-Verlag.

Basseville, M. et al. 2001. Output only subspace-based structural identification: from theory to industrial testing practice, Trans. of the ASME 123, p.668-676.

Carden, E. P. and Brownjohn, M. W. 2008. ARMA modeled time-series classification for structural health monitoring of civil structure, Mechanical Systems and Signal Processing 22, p.295-314.

Gevers, M. 2006. A personal view on the development of system identification a 30-year journey through an exciting field, IEEE Control System Magazine 26(6) :p.93-105.

Garibaldi, L. et al. 1998. ARMAV techniques for traffic excited bridges, ASME Journal of vibration and Acoustics 120, p.713-718.

Juang, J. N. 1994. Applied System Identification, Prentice hall PTR.

Lardies, J. 1998. State-space identification of vibrating systems from multi-output measurements, Mechanical Systems and Signal Processing 12(4): p.543-558.

Magalhães, F. Á. and Chunha, E. C. 2009. Online automatic identification of the modal parameters of a long span arch bridge, Mechanical Systems and Signal Processing 123: p.316-329.

Overschee, P. V. and Moor, B. D. 1996. Subspace identification for linear systems, Kluwer Academic Publishers.

Papakos, V. and Fassois, S. D. 2003. Multi channel identification of Aircraft skeleton structures under unobservable excitation, A vector AR/ARMA framework, Mechanical Systems and Signal Processing 17(6): p.1271-1290.

Peeters, B. and Roeck, G. D. 2001. Stochastic system identification for operational modal analysis: a review, Journal of Dynamic System, Measurement and Control 123:p.659-667.